

Technical Note

Seismic ground response analysis of unsaturated soil deposits

M. Biglari^{1,*}, I. Ashayeri¹

Received: 2012/04/8, Revised: 2012/07/16, Accepted: 2012/11/19

Abstract

Seismic ground motion is profoundly affected by geometrical and mechanical properties of soil deposits overlaying bedrock. Local seismic ground response of saturated soil deposits was studied in literature by applying the effects of soil stress state and index properties on the strain-dependent normalized shear modulus reduction, G/G_0 , and damping ratio, D , curves in an equivalent linear analysis. However, experimental investigations revealed that, G_0 , G/G_0 , and D of unsaturated soils are influenced by stress state as well as suction. This study presents the results of linear and equivalent linear seismic ground response analysis of unsaturated soil deposits incorporating suction effects on G/G_0 and D curves. Seismic ground response analyses were done with the computer program EERA for three sets of soil profiles, which are included in saturated, constant and linearly variable suction unsaturated soil deposits. The results of current study present the magnitude of variation in natural frequency, amplification ratio and spectral acceleration of unsaturated soil deposits.

Keywords: Unsaturated soil, Soil dynamics, Equivalent-linear, Seismic ground response analysis, EERA.

1. Introduction

Local soil conditions have profound influence on the ground response during earthquakes, which is modelled through direct non-linear elasto-plastic [1-4] or equivalent-linear elastic ground response analysis [5-7]. In spite of its theoretical shortcomings, the latter has become the major tool in practical engineering applications due to its simplicity. The equivalent-linear analysis consists of modifying normalized shear modulus G/G_0 , and damping ratio D , of a visco-elastic soil model with shear strain level, γ . Usually the strain-dependent normalized shear modulus reduction ($G/G_0-\gamma$) and damping ratio ($D-\gamma$) curves are obtained by laboratory tests. However, mathematical functions were presented for $G/G_0-\gamma$ and $D-\gamma$ in terms of stress state and index properties of saturated soils based on the numerous experiments by various investigators [8-10].

Experimental investigations revealed that initial shear modulus G_0 , of unsaturated soils is influenced by stress state as well as suction [11-16]. Furthermore, a recent investigation on the measurements of shear modulus of an unsaturated soil at wider shear strain range by suction-controlled cyclic tri-axial apparatus shows that $G-\gamma$ and $D-\gamma$

curves are influenced by the suction levels too [17]. On the basis of this experimental evidence, the empirical equations proposed by [10] for $G/G_0-\gamma$ and $D-\gamma$ curves of saturated soils were modified by [18] to take into the account the influence of the suction level in addition to stress state and index properties for unsaturated soils. [19] investigated the effect of suction on the linear seismic ground response of unsaturated soils which only takes into the account the influence of suction on the shear wave velocity or initial shear modulus. They have presented the results in terms of amplification ratio of surface motion in the frequency domain and concluded that the natural frequency of soil deposit significantly increases with suction increase and the maximum amplification ratio is substantially reduced.

This study presents the results of 1D- linear and equivalent linear seismic ground response analysis of unsaturated soil deposit not only by considering the effects of suction variation on the shear wave velocity V_s , or initial shear modulus G_0 , but also by taking into the account the dependency of $G/G_0-\gamma$ and $D-\gamma$ to the suction level. Seismic ground response analyses were done with the computer program EERA (Equivalent-linear Earthquake site Response Analyses [7]) for six soil profiles and three time histories of acceleration. The results are discussed in terms of comparison between the natural frequency and amplification ratio of soil deposits as well as spectral acceleration of the ground motion at surface and bedrock.

* Corresponding Author: m.biglari@razi.ac.ir
1 Assistant Professor, Civil Engineering Department, School of Engineering, Razi University, Kermanshah, Iran

2. Soil profiles

Six soil profiles were considered in this study within three sets of analysis. The first set compares two soil profiles P1 and P2 of lean clay deposit 24 meters deep overlaying the bedrock. Table 1 presents the variation of suction, shear wave velocity, and total unit weight of different layers of the soil profiles P1 and P2. Soil profile P1 is formed of a two meters of saturated soil layer over the bedrock that is overlaid by 22 meters of unsaturated soil with variable suctions. The unsaturated soil deposit of P1 was divided into 6 layers of constant suction varying linearly from zero to 250 kPa. On the other hand, soil profile P2 is formed of 24 meters of saturated soil deposit overlaying the bedrock that is divided into 7 layers of variable shear wave velocity and unit weight.

The second set of analysis compares three soil profiles P3, P4, and P5. Table 2 presents the variation of suction, shear wave velocity, and total unit weight of the different layers of the soil profiles P3, P4, and P5. Soil profile P3 is formed of 24 meters of saturated soil deposit overlaying the bedrock that is divided into 6 layers with variable shear wave velocity and unit weight. Soil profile P4 is formed of 24 meters of unsaturated soil deposit with constant suction of 150 kPa overlaying the bedrock and is divided into 6 layers with variable shear wave velocity and unit weight. Soil profile P5 is formed of 24 meters of unsaturated soil deposit with constant suction of 300 kPa overlaying the bedrock and again is divided into 6 layers with variable shear wave velocity and unit weight.

The third set compares two soil profiles P5 and P6. Soil profile P6 is an imaginary profile specifically similar to P5

Table 1 Description of soil profiles of the first set of analysis

Layer	Thickness (m)	Profile					
		P1			P2		
		s^a (kPa)	V_s^b (m/sec)	γ^c (kN/m ³)	s (kPa)	V_s (m/sec)	γ (kN/m ³)
1	+	250	139	13.43	0	133	19.30
2	+	200	139	13.63	0	133	19.30
3	+	150	170	14.10	0	130	19.30
4	+	100	107	13.13	0	143	19.37
5	+	50	201	16.19	0	134	19.61
6	?	0	193	19.66	0	164	19.63
7	?	0	300	19.93	0	172	19.77
8	Bed Rock		1319.1	33.03		1319.1	33.03

^a s : suction, ^b V_s : shear wave velocity, ^c γ : unit weight

Table 2 Description of soil profiles of the second set of analysis

Layer	Thickness (m)	Profile								
		P3			P4			P5 and P6		
		s (kPa)	V_s (m/sec)	γ (kN/m ³)	s (kPa)	V_s (m/sec)	γ (kN/m ³)	s (kPa)	V_s (m/sec)	γ (kN/m ³)
1	+	0	133	19.30	150	139	13.70	300	176	13.30
2	+	0	133	19.30	150	139	13.70	300	176	13.30
3	+	0	130	19.30	150	170	14.30	300	103	13.00
4	+	0	143	19.37	150	103	14.60	300	203	14.30
5	+	0	134	19.61	150	203	13.30	300	119	14.30
6	+	0	164	19.71	150	119	13.30	300	233	14.70
7	Bed Rock		1319.1	33.03		1319.1	33.03		1319.1	33.03

with the same shear wave velocity and unit weight given in Table 2. The difference between these two profiles is in the using different $G/G_0-\gamma$ and $D-\gamma$ curves during equivalent linear response analysis. More details on this set of analysis is given in Sec. 4.

The shear wave velocities of the soil layers of P1 to P5 were calculated from the model for initial shear modulus of unsaturated soils calibrated for the current material [15-16].

3. Modulus reduction and damping ratio curves

In order to generate $G/G_0-\gamma$ and $D-\gamma$ curves, the empirical equations presented by [18] were used. Equations (1) to (6) represent the empirical equations of G/G_0 :

$$\frac{G}{G_0} = A(\gamma, \xi, PI) \left(\frac{p''}{p_{atm}} \right)^{n(\gamma, PI) - n_0} \quad (1)$$

$$A(\gamma, \xi, PI) = 0.5 \left[1 + \tanh \left\{ \ln \left(\frac{0.00005 + 0.0167 \xi^{12.16} + f(PI)}{\gamma} \right)^{(0.26 + 3.61 \xi^{11.6})} \right\} \right] \quad (2)$$

$$f(PI) = \begin{cases} 0.0 & \text{for } PI = 0 \quad (\text{sandy soils}) \\ 3.37 \times 10^{-6} PI^{1.404} & \text{for } 0 < PI \leq 15 \quad (\text{low plastic soils}) \\ 7.0 \times 10^{-7} PI^{1.976} & \text{for } 15 < PI \leq 70 \quad (\text{medium plastic soils}) \\ 2.7 \times 10^{-3} PI^{1.115} & \text{for } 70 < PI \quad (\text{high plastic soils}) \end{cases} \quad (3)$$

$$n(\gamma, PI) - n_0 = 0.272 \left[1 - \tanh \left\{ \ln \left(\frac{0.000556}{\gamma} \right)^{0.4} \right\} \right] e^{-0.0145 PI^{1.3}} \quad (4)$$

$$p'' = (p - u_a) + S_r(u_a - u_w) \quad (5)$$

$$\xi = f(s) \cdot (1 - S_r) \quad (6)$$

where $A(\gamma, \xi, PI)$ is stiffness index ratio defined as Eq. (2), p_{atm} is the atmospheric pressure, p'' is the average skeleton stress defined as Eq. (5), $n(\gamma, PI)$ is a stiffness coefficient accounts for the effect of p'' on stiffness, n_0 is a stiffness coefficient accounts for the effect of p'' on stiffness in small strain range, p is average total stress, S_r is degree of saturation, u_a is air pressure, u_w is water pressure, s is matric suction equal to $(u_a - u_w)$, ξ is the bonding variable defined as Eq. (6) where $f(s)$ is a function that depends on the size of the particles and the value of the water surface tension. The value of $f(s)$ was considered equal to 1 for the range of suctions in this study.

Equation (7) represents the damping ratio as a function of G/G_0 .

$$D = f\left(\frac{G}{G_0}\right)A(PI) = \left[0.358 \left\{ -0.11 \left(\frac{G}{G_0}\right)^2 - 0.587 \left(\frac{G}{G_0}\right) + 1 \right\} \right] \left[\frac{1 + e^{-0.0145 PI^{1.3}}}{2} \right] \quad (7)$$

Figures 1 to 6 present the generated $G/G_0-\gamma$ and $D-\gamma$ for layers of soil profiles P1 to P6, respectively. The soil plasticity index PI, was considered equal to 12%, and appropriate suction and confining pressure of each layer of the soil profiles were used.

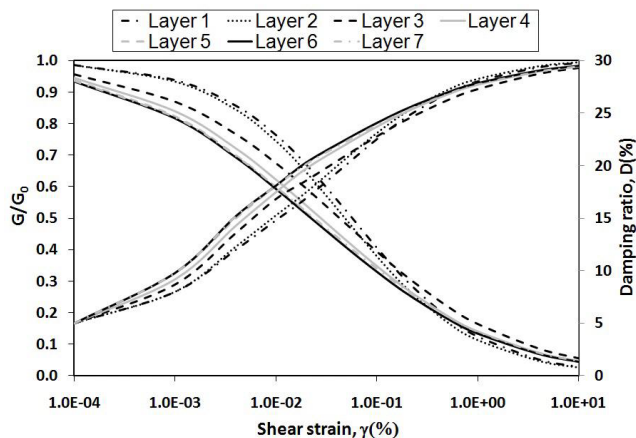


Fig. 1 $G/G_0-\gamma$ and $D-\gamma$ curves of layers of P1

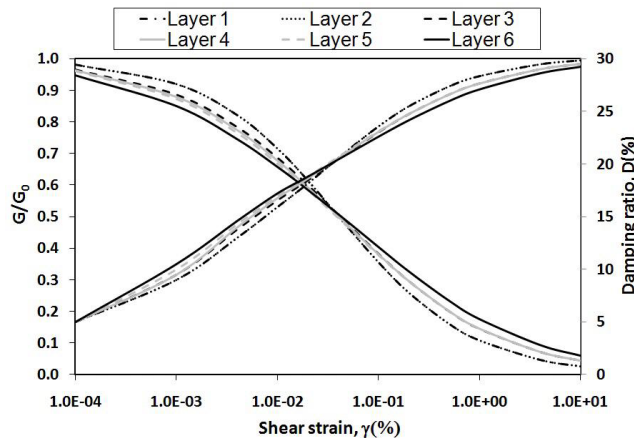


Fig. 4 $G/G_0-\gamma$ and $D-\gamma$ curves of layers of P4

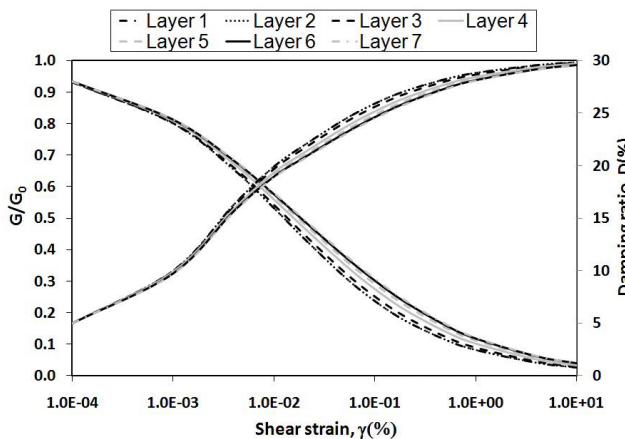


Fig. 2 $G/G_0-\gamma$ and $D-\gamma$ curves of layers of P2

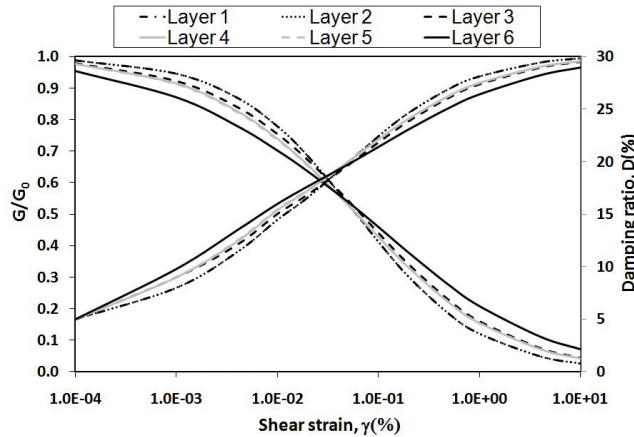


Fig. 5 $G/G_0-\gamma$ and $D-\gamma$ curves of layers of P5

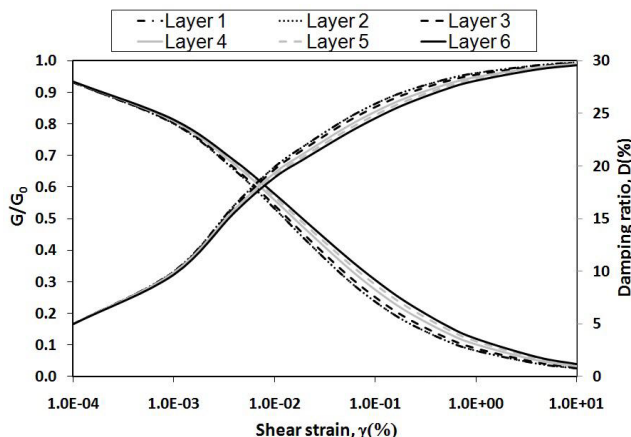


Fig. 3 $G/G_0-\gamma$ and $D-\gamma$ curves of layers of P3

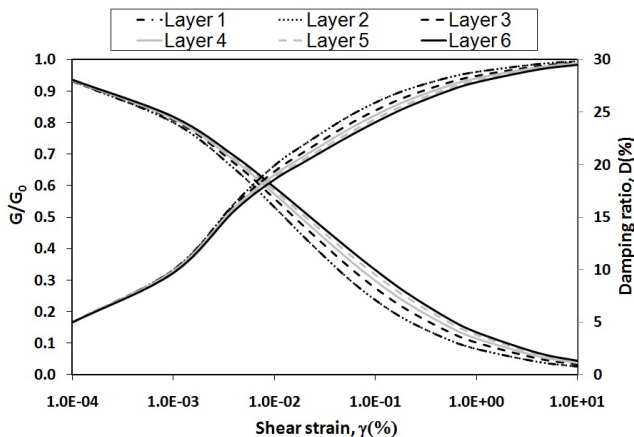


Fig. 6 $G/G_0-\gamma$ and $D-\gamma$ curves of layers of P6

4. Ground response analysis

Seismic ground response analyses were done with the computer program EERA [7] for the six soil profiles P1 to P6. EERA is a modern implementation of the well-known concepts of equivalent linear earthquake site response analysis applied in SHAKE [20]. The soil profiles are subjected to the input ground motion from the bedrock that is specified as an out-crop motion. To avoid dependency of the ground response to the input motion,

three accelerographs were used in the analyses. These three input motions are the acceleration time history of Loma Prieta 1989, Kobe 1995, and Chichi 1999 earthquakes (Records P0782, P1043 & P1116 at <http://peer.berkeley.edu/smcat/>). The ground motions are normalized to a target peak acceleration of 0.1g.

The comparisons between Peak Ground Acceleration (PGA) at surface, amplification ratio, and first natural frequency of each soil profile are presented in Table 3 for the three ground motions. The first natural frequency increases from 0.8 Hz for P2 to 1.4 Hz for P1 and it varies from 0.8 Hz for P3 to 1.6 Hz for P5 by increasing suction. The PGA of the motion at surface of the all profiles is larger than the bedrock motion and this is more significant at the unsaturated profiles.

Figure 7 shows amplification between the surface motion and the base motion at varying frequencies for P1 and P2 for Loma Prieta earthquake. The increase in the natural frequency with suction increase reasonably can be assigned to the increase of shear modulus by suction. However, the variation of

amplification ratio is related to the admittance ratio between the soil and the bedrock, which resulted into increasing amplification ratio by increasing suction.

To provide comparison of the effects of non-linearity, series of linear analyses were performed for P3 to P5 which, the results are presented in Figures 8 to 10. It is clear that non-linearity has influenced the results significantly in terms of both amplification ratio and natural frequency.

In order to evaluate the magnitude of influence of using suction dependent modulus reduction and damping ratio curves on the natural frequency and amplification ratio third set of analysis was performed. This set contains equivalent linear seismic ground response analyses of P5 and P6 subjected to Loma Prieta earthquake. As it was previously explained, these two profiles are specifically similar except that P5 uses those modulus reduction and damping ratio curves obtained from Eqs. (1) and (7) by considering $s = 300$ kPa (Figure 5), while P6 uses those curves obtained from Eqs. (1)

Table 3 Comparison between PGA values of bed rock and surface of the all profiles

Profile	PGA (g), Amplification Factor, 1 st natural frequency (Hz)		
	Loma Prieta	Kobe	Chichi
P1	0.146, 2.50, 1.4		
P2	0.113, 2.29, 0.8		
P3	0.113, 2.29, 0.8	0.117, 2.30, 0.8	0.104, 2.19, 0.8
P4	0.148, 2.61, 1.4	0.155, 2.56, 1.4	0.154, 2.59, 1.4
P5	0.146, 2.71, 1.6	0.154, 2.69, 1.6	0.175, 2.69, 1.6
P6	0.141, 2.44, 1.4		

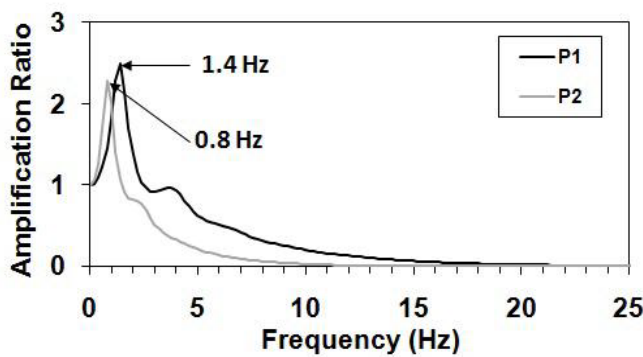


Fig. 7 Amplification functions of P1 and P2

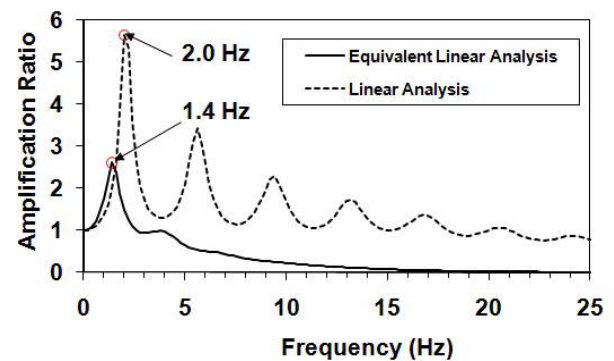


Fig. 9 Amplification functions of P4 in different analysis

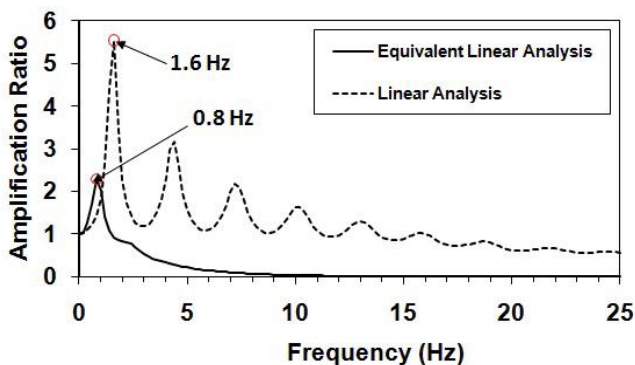


Fig. 8 Amplification functions of P3 in different analysis

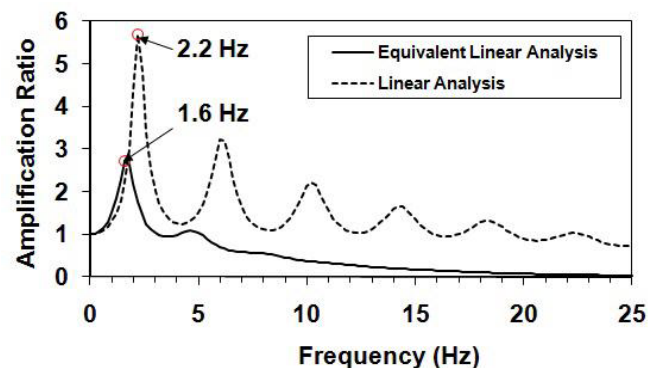


Fig. 10 Amplification functions of P5 in different analysis

and (7) by considering $s = 0$ (Figure 6). The first natural frequency of P6 is equal to 1.4 Hz which is less than 1.6 Hz as obtained for P5. Figure 11 show the results of this analysis. It expresses that if inappropriate modulus reduction and damping ratio curves are used, the natural frequency of the unsaturated soil deposit is underestimated.

Another index to seismic hazard of buildings and structures is response spectral acceleration curve. Spectral acceleration, S_a , is the maximum acceleration of a single degree of freedom oscillator with different natural frequencies but unique damping ratio. Figures 12 to 15 compare the S_a with 5% damping ratio at the ground surface of P1 to P5 with the one at bedrock.

Shift of S_a to the lower frequencies (higher periods) at the surface of the saturated profiles (P2 and P3) is observed. However, S_a of the surface ground motion of unsaturated

profiles (P1, P4, and P5) is considerably different with the ones of saturated profiles (P2 and P3) and the bed rock. The results show that the S_a increases by suction increase for high frequencies (periods less than 1 sec). This is very important and should be noticed in seismic design of structures on the unsaturated soil deposits particularly for short buildings with high natural frequency.

5. Summary and conclusions

The aim of this study was to perform 1D- linear and equivalent linear site response analysis by considering the influence of suction on the shear wave velocity, shear modulus reduction and damping ratio curves. Three sets of analyses compare the response of three unsaturated soil profiles with the saturated ones due to three earthquakes. It came out with the following conclusions for the selected soil profiles.

- The natural frequency of the soil profile increases as the suction increases. This will attract the attentions to the suitable natural frequency of the buildings on the unsaturated soil deposits.
- The ground motions were amplified at the surface for all of the saturated (P2 and P3) and unsaturated profiles (P1, P4 & P5). However, the combined conditions considered in the soil profiles showed that the amplification ratio is slightly larger at unsaturated soils that may not to be a general behaviour.
- Response spectral accelerations calculated for damping ratio of 5%, show that the response of the structures on the unsaturated soil profiles are more severe than saturated ones, particularly at higher frequencies.

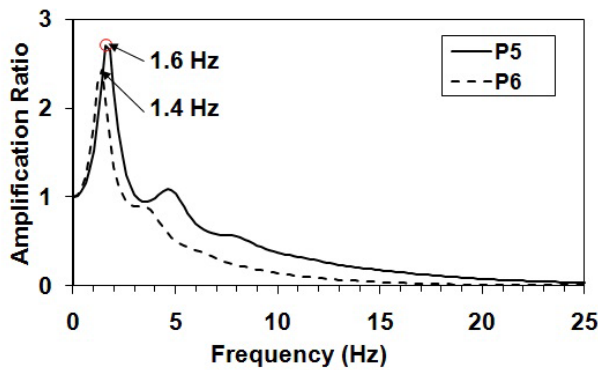


Fig. 11 Amplification functions of P5 and P6 in equivalent linear analysis

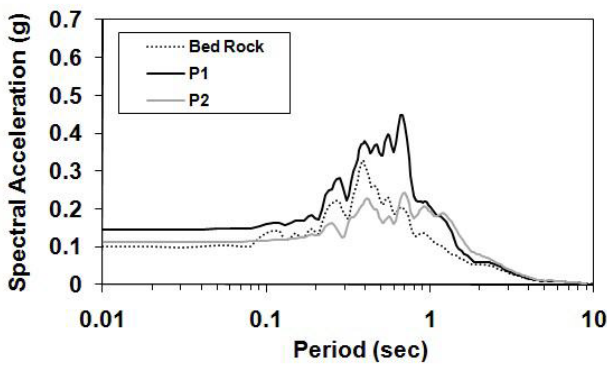


Fig. 12 S_a of P1 and P2 for Loma Prieta

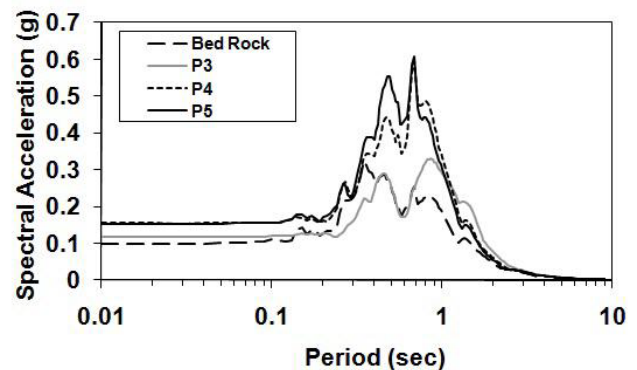


Fig. 14 S_a of P3, P4, and P5 for Kobe

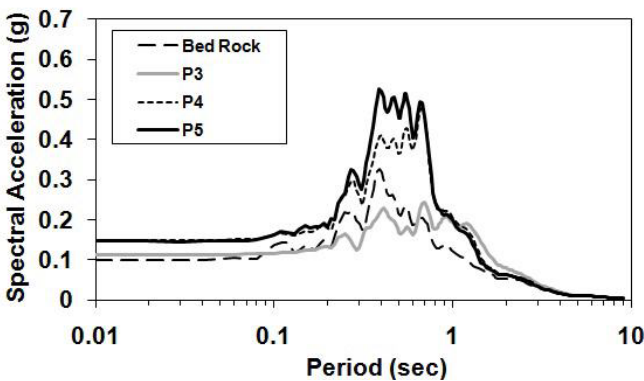


Fig. 13 S_a of P3, P4, and P5 for Loma Prieta

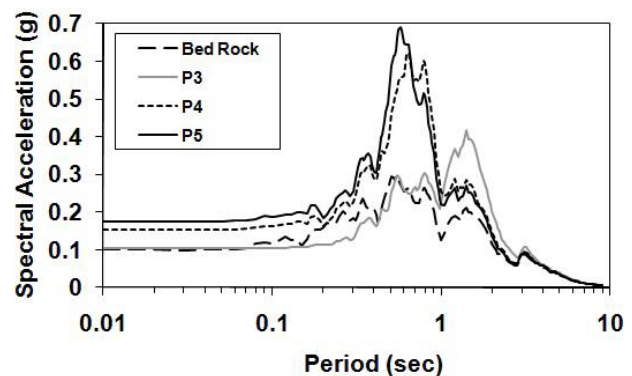


Fig. 15 S_a of P3, P4, and P5 for Chichi

Acknowledgment: The authors wish to acknowledge the support of the Razi University through research grant Code: 36471.

References

- [1] Lee M.K.W and Finn W.D.L. DESRA-2, Dynamic Effective Stress Response Analysis of Soil Deposits With Energy Transmitting Boundary Including Assessment of Liquefaction Potential. Software manual, Faculty of Applied Science, University of British Columbia, Vancouver, Canada (1978).
- [2] Prevost J.H. DYNA1D: A Computer Program for Nonlinear Seismic Site Response Analysis- Technical Documentation. Multidisciplinary Center for Earthquake Engineering Research, Report NCEER-89-0025 (1989).
- [3] Hashash Y.M.A. and Park D. Non-linear one-dimensional seismic ground motion propagation in the Mississippi embayment. Engineering Geology, 2001; 62(1-3): 185-206.
- [4] Hashash Y.M.A. and Park D. Viscous damping formulation and high frequency motion propagation in nonlinear site response analysis. Soil Dynamics and Earthquake Engineering, 2002; 22(7): 611-624.
- [5] Idriss I.M. and Seed H.B. Seismic Response of Horizontal Soil Layers. Journal of the Soil Mechanics and Foundations Division, ASCE, 1968; 94(4): 1003-1031.
- [6] Idriss I.M and Sun J.I. User's Manual for SHAKE91. Center for Geotechnical Modeling, Department of Civil Engineering, University of California, Davis (1992).
- [7] Bardet J.P., Ichii K. and Lin C.H. EERA, A computer program for Equivalent linear Earthquake site Response Analysis of layered soils deposits. Software Manual, University of Southern California, Los Angeles (2000).
- [8] Seed H.B., Wong R.T., Idriss I.M. and Tokimatsu K. Moduli and damping factors for dynamic analyses of cohesionless soils. Journal of Geotechnical Engineering, ASCE, 1986; 112(11): 1016-1032.
- [9] Vucetic M. and Dobry R. Effect of soil plasticity on cyclic response. Journal of Geotechnical Engineering, ASCE, 1991; 117(1): 89-107.
- [10] Ishibashi I. and Zhang X. Unified dynamic shear moduli and damping ratios of sands and clays. Soils and Foundations, 1993; 33(1): 182-191.
- [11] Mancuso C., Vassallo R. and d'Onofrio A. Small strain behavior of a silty sand in controlled-suction resonant column – torsional shear tests. Canadian Geotechnical Journal, 2002; 39: 22– 31.
- [12] Vassallo R., Mancuso C. and Vinale F. Effects of net stress and suction history on the small strain stiffness of a compacted clayey silt. Canadian Geotechnical Journal, 2007; 44: 447- 462.
- [13] Vassallo R., Mancuso C. and Vinale F. Modelling the influence of stress–strain history on the initial shear stiffness of an unsaturated compacted silt. Canadian Geotechnical Journal, 2007; 44: 463- 472.
- [14] Ng C.W.W. and Yung S.Y. Determination of the anisotropic shear stiffness of an unsaturated decomposed soil. Géotechnique, 2008; 58(1): 23–35.
- [15] Biglari M., Mancuso C., d'Onofrio A., Jafari M.K. and Shafiee

- A. Modelling the initial shear stiffness of unsaturated soils as a function of the coupled effects of the void ratio and the degree of saturation. Computers and Geotechnics, 2011; 36: 709-720.
- [16] Biglari M., d'Onofrio A., Claudio M., Jafari M.K. and Shafiee A. Small strain stiffness of Zeno kaolin in unsaturated conditions, Canadian Geotechnical Journal, 2012; 49(3): 311-322 .
- [17] Biglari M., Jafari M.K., Shafiee A., Mancuso C. and d'Onofrio A. Shear Modulus and Damping Ratio of Unsaturated Kaolin Measured by New Suction-Controlled Cyclic Triaxial Device. Geotechnical Testing Journal, ASTM, 2011; 34(5).
- [18] Biglari M. and Ashayeri I. An empirical model for shear modulus and damping ratio of unsaturated soils. Proc. 5th Asia-Pacific Conf. on Unsaturated Soils, Pataya, Thailand (2012).
- [19] d'Onza F., d'Onofrio A. and Mancuso C. Effects of unsaturated soil state on the local seismic response of soil deposits. Proc. 1st European Conf. on Unsaturated Soils, Durham, UK, 2008; 531-536.
- [20] Schnabel P.B., Lysmer J. and Seed H.B. SHAKE: A Computer Program for Earthquake Response Analysis of Horizontally Layered Sites, Report No. UCB/EERC-72/12, Earthquake Engineering Research Center, University of California, Berkeley, December, (1972) 102p.

Notations

The following symbols are used in this paper:

G_0 = initial shear stiffness or initial shear modulus
 G = shear stiffness or shear modulus
 G/G_0 = shear modulus reduction
 D = damping ratio
 V_s = shear velocity
 γ = shear strain
 PI = plasticity index
 A = stiffness index
 n = stiffness coefficient accounting for the effect of p'' on the stiffness
 n_0 = stiffness coefficient accounting for the effect of p'' on the stiffness in small strain range
 p_{atm} = atmospheric pressure
 p = average total stress
 p'' = average skeleton stress
 u_a = air pressure
 u_w = water pressure
 s = matric suction
 ζ = bonding variable
 S_r = degree of saturation
 ρ = unit weight
 S_a = spectral acceleration
PGA = Peak Ground Acceleration
EERA = Equivalent linear Earthquake Response Analysis